ACS OMEGA

http://pubs.acs.org/journal/acsodf

Article

Hydroxyethyl Starch–Bovine Hemoglobin Conjugate as an Effective Oxygen Carrier with the Ability to Expand Plasma

Wenying Yan,[#] Ming Sheng,[#] Weili Yu, Lijuan Shen, Jinming Qi, Hong Zhou, Tao Hu,[*] and Lian Zhao[*]

Cite This: *ACS Omega* 2023, 8, 11447−11456

Read Online

ACCESS | Metrics & More | Article Recommendations

ABSTRACT: Hemorrhagic shock leads to intravasal volume deficiency, tissue hypoxia, and cellular anaerobic metabolism. Hemoglobin (Hb) could deliver oxygen for hypoxic tissues but is unable to expand plasma. Hydroxyethyl starch (HES) could compensate for the intravasal volume deficiency but cannot deliver oxygen. Thus, bovine Hb (bHb) was conjugated with HES (130 kDa and 200 kDa) to develop an oxygen carrier with the ability to expand plasma. Conjugation with HES increased the hydrodynamic volume, colloidal osmotic pressure, and viscosity of bHb. It slightly perturbed the quaternary structure and heme environment of bHb. The partial oxygen pressures at 50% saturation (P_{50}) of the two conjugates (bHb-HES130 and bHb-HES200) were 15.1 and 13.9 mmHg, respectively. The two conjugates showed no apparent side effects on the morphology and rigidity, hemolysis, and platelet aggregation of red blood cells of Wistar rats. Thus, bHb-HES130 and bHb-HES200 were expected to function as an effective oxygen carrier with the ability to expand plasma.

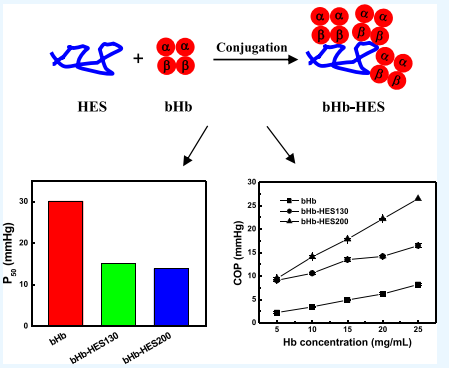

1. INTRODUCTION

Hemorrhagic shock can lead to tissue hypoxia, cellular respiration into anaerobic metabolism, and intravasal volume deficiency, which alter the normal physiological function.[1,2] Blood transfusion is an effective method to alleviate the hemorrhagic shock by its ability to deliver oxygen, expand the blood volume, and improve the microcirculation.[3,4] However, blood transfusion suffers from several disadvantages, such as cross-matching, pathogen-borne diseases (e.g., AIDS and hepatitis C), allergic reactions, and the shortage of blood supply.[5]

Plasma expanders have been used in emergent transfusion for serious blood and fluid loss, circulation stabilization, and blood dilution.[6,7] Crystalloid solutions (e.g., stroke-physiological saline solution) and colloid solutions (e.g., dextran, gelatin, albumin, and hydroxyethyl starch (HES)) have been clinically used as plasma expanders.[8,9] Compared with crystalloid solutions, colloid solutions effectively maintain the functional capillary density and expand the blood volume and osmotic pressure thereby improving the microcirculation of tissues in hemorrhagic shock.[10,11]

HES is a highly branched and semi-synthetic amylopectin consisting of ether-linked hydroxyethyl groups.[11,12] As a colloid solution, HES is an effective plasma expander with a wide application in clinical therapy of intravasal volume deficiency.[13,14] However, clinical therapy with HES results in allergic reactions, bleeding defects, and platelet damage.[15] The clinical defects of HES depend on the M_w and the degree of substitutes. For example, HES450 (450 kDa) and HES700 (700 kDa) lead to bleeding complications and pruritus.[16] HES70 (70 kDa) shows a low volume expansion ability for its rapid renal elimination, whereas HES130 (130 kDa) and HES200 (200 kDa) induces severe tissue hypoxia.[17] Moreover, hypoxic shock is not fully alleviated by transfusion of plasma expanders (e.g., HES) due to the fact that they cannot provide oxygenation for the hypoxic tissues.

Hemoglobin (Hb), a tetrameric protein, could deliver and release oxygen in a cooperative manner.[18] Hb in red blood cells (RBCs) could act as an oxygen carrier to alleviate tissue hypoxia brought by hemorrhagic shock.[19] However, Hb suffers from tetrameric dissociation, renal toxicity, and a short plasma retention time in vivo due to its relatively small molecular size and tetrameric dissociation.[20,21] Hb-based oxygen carriers (HBOCs) overcome the disadvantages of Hb for their large molecular size and could deliver oxygen to hypoxic tissues.[22,23] Several HBOCs have been developed for surgery or emergency transfusion, including polymerized Hb, PEGylated Hb, and dextran−Hb conjugates (dex-Hb).[24] Polymerized Hb was prepared by cross-linking tetrameric Hb with glutaraldehyde. PEGylated Hb and dex-Hb were prepared by conjugation of Hb with polyethylene glycol (PEG) and dextran.[25]

Received: January 14, 2023
Accepted: March 8, 2023
Published: March 16, 2023

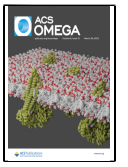

https://doi.org/10.1021/acsomega.3c00275
ACS Omega 2023, 8, 11447−11456

In order to treat hemorrhagic shock that induces tissue hypoxia and intravasal volume deficiency, a solution with the ability to deliver oxygen and expand the blood volume was highly desired. However, some HBOCs (e.g., polymerized Hb) could not expand the blood volume for their low colloid osmotic pressure (COP).[26,27] The PEGylated Hb and dex-Hb could act as an oxygen carrier and plasma expander for their ability to deliver oxygen and expand the blood volume with the high COP.[28,29] However, the high COP of the PEGylated Hb (>100 mmHg at 40 mg/mL) might lead to intracellular fluid loss and hypertonic dehydration.[29] Moreover, PEGylation of proteins could elicit anti-PEG immunity.[30,31] In addition, dex-Hb may lead to allergies and renal failure.[32]

Conjugation of HES with Hb is an effective method to solve the problems of HES and Hb.[33,34] It is expected that the conjugate can deliver and release oxygen to treat the hypoxic tissues due to the presence of Hb. The conjugate can also compensate for the intravasal volume deficiency with the presence of HES. Bovine Hb (bHb) shows 85% homology to human adult Hb (HbA) and has no quantity constraints with its ample resource and controllable quality.[35] HES130 and HES200 both have a moderate M_w and less side effects.

In the present study, two bHb-HES conjugates (bHb-HES130 and bHb-HES200) were prepared by conjugation of bovine Hb (bHb) with HES130 and HES200, respectively. The structure, heme environment, and oxygen delivery properties of the conjugates were measured to evaluate their effectiveness as oxygen carriers. The COP and viscosity of the conjugates were measured to evaluate their effectiveness as plasma expanders. The effects of the conjugates on the morphology, hemolysis, and platelet aggregation of red blood cells of Wistar rats were determined.

2. MATERIALS AND METHODS

2.1. Materials. HES with a M_w of 130 kDa and degree of substitution of 0.4 (HES130), HES with a M_w of 200 kDa and degree of substitution of 0.5 (HES200), sodium cyanoborohydride, 8-anilino-1-naphthalene sulfonic salt (ANS), sodium periodate, 4,4′-dithiodipyridine (4-PDS), and adenosine diphosphate (ADP) were ordered from Sigma. All other reagents were of analytical grade.

2.2. Purification of bHb. Bovine blood erythrocytes were obtained freshly from a local slaughterhouse. The blood was centrifuged at 10,000*g* for 5 min at 4 °C to remove the serum. The pellet was resuspended in PBS buffer (pH 7.4) at the original volume. This process was repeated three times to remove as much serum as possible. The remaining red blood cells were then lysed overnight at 4 °C in an equal volume of distilled water. The solution was then centrifuged at 10,000*g* for 60 min at 4 °C to remove cell debris. The solution was dialyzed against 50 mM Tris−HCl buffer (pH 8.5) and loaded on a Q Sepharose High Performance column (2.6 cm × 20 cm, GE Healthcare, USA).[36] The column was equilibrated with five column volumes (CVs) of 50 mM Tris−HCl buffer (pH 8.5) and eluted by a pH gradient (pH 8.5−6.5) in 50 mM Tris−HCl buffer. The peak corresponding to bHb was fractionated.

2.3. Preparation and Purification of the Conjugates. HES130 (50 mg/mL) and HES200 (50 mg/mL) were oxidized by 20 mM sodium meta-periodate in 20 mM sodium acetate buffer (pH 5.6). The mixtures were incubated at room temperature for 30 min in the dark and terminated by addition of excessive ethylene glycol followed by extensive dialysis against PBS buffer (pH 7.4). bHb was incubated with the oxidized HES130 and $NaCNBH_3$ at a molar ratio of 4:3:300 at 4 °C for overnight. Glycine was added at a glycine−Hb molar ratio of 20:1 to terminate the reaction and obtain the bHb-HES130 conjugate (bHb-HES130). The bHb-HES200 conjugate (bHb-HES200) was prepared essentially in the same way as bHb-HES130 except that HES200 was used.

A Superdex 200 column (2.6 cm × 60 cm, GE Healthcare, USA) was used to purify the conjugates based on size exclusion chromatography (SEC). The column was equilibrated and eluted by PBS buffer (pH 7.4) at a flow rate of 2.0 mL/min. The effluent was monitored at 280 nm. Due to the difference in the size of the conjugates, Hb, and HES, the three components in the reaction mixtures were well separated by the column. The peaks corresponding to the two conjugates were fractionated.

2.4. SDS-PAGE Analysis. SDS-PAGE analysis of bHb-HES130 and bHb-HES200 was performed on a 12% polyacrylamide gel under a reducing (5% *v*/*v*, *β*-mercaptoethanol) condition. The gel was stained by Coomassie blue R-250.

2.5. Quantitative Assay. The concentrations of oxy-, deoxy-, and methemoglobin were calculated from their absorbance at three wavelengths (630, 576, and 560 nm).[37] The total bHb concentration was obtained from the summation of the concentrations of the three components. The HES contents of the conjugates were determined by the phenol-sulfuric acid method.[38] The bHb/HES molar ratios of the conjugates were thus calculated by comparison of the bHb and HES contents.

2.6. Size Exclusion Chromatography Analysis. bHb-HES130 and bHb-HES200 were analyzed by an analytical Superose 6 column (1 cm × 30 cm, GE Healthcare, USA) at room temperature. The column was extensively equilibrated and eluted by PBS buffer (pH 7.4) at a constant flow rate of 0.5 mL/min. The effluent was detected at 280 nm.

2.7. Thiol Reactivity. The thiol reactivities of bHb-HES130 and bHb-HES200 were estimated by measuring the conversion of 4-PDS to 4-thiopyridone at 324 nm as a function of incubation time.[39] The thiol groups of Cys-93(β) in bHb-HES130 and bHb-HES200 were calculated by evaluation of the 4-thiopyridone content.

2.8. Circular Dichroism Spectroscopy. A J-810 spectropolarimeter (Jasco, Japan) was used to record the circular dichroism (CD) spectra of bHb-HES130 and bHb-HES200 at 25 °C. For the near-UV spectra (480−260 nm), bHb-HES130 and bHb-HES200 were both at a protein concentration of 2.0 mg/mL in 20 mM sodium phosphate buffer (pH 7.4). The spectra were obtained with an average of three repeated scans using a cuvette with a 1 mm path length. The molar ellipticity (θ) was expressed in degree square-centimeter per decimole on a heme basis.

2.9. Dynamic Light Scattering. The molecular sizes of bHb-HES130 and bHb-HES200 were determined by dynamic light scattering based on a Zetasizer Nano ZS (Malvern Panalytical, UK). bHb-HES130 and bHb-HES200 were both at a protein concentration of 1.0 mg/mL in 20 mM sodium phosphate buffer (pH 7.4).

2.10. Extrinsic Fluorescence Measurement. bHb-HES130 and bHb-HES200 were mixed with 10-fold molar ANS at a final protein concentration of 0.1 mg/mL in 20 mM sodium phosphate buffer (pH 7.4). The resultant samples were determined by extrinsic fluorescence spectroscopy using an F-4500 fluorescence spectropolarimeter (Hitachi, Japan). The

https://doi.org/10.1021/acsomega.3c00275
ACS Omega 2023, 8, 11447−11456

emission spectra were excited at 350 nm and recorded from 400 to 650 nm. The excitation and emission slit widths were 10 and 20 nm, respectively.

2.11. Oxygen Affinity. Oxygen equilibrium curves of bHb-HES130 and bHb-HES200 were recorded with a Hemox analyzer (TCS Scientific, USA) at 37 °C, as described elsewhere.[40] bHb, bHb-HES130, and bHb-HES200 were all at a protein concentration of 1.5 mg/mL in the Hemox buffer. The P_{50} values were obtained directly from the curves. The Hill coefficient (n) was calculated from the Hill plot ($\log Y/(1-Y)$ vs $\log P$) where Y was the fractional saturation of Hb with oxygen and P was the oxygen pressure in millimeters of mercury (mmHg).

2.12. Bohr Effect. The oxygen equilibrium curves of bHb-HES130 and bHb-HES200 were measured at a pH range of 7.2−7.6. The P_{50} and Hill coefficient of bHb-HES130 and bHb-HES200 were obtained to evaluate their Bohr effects.

2.13. UV−Vis Spectroscopy. The UV−vis spectra (300−700 nm) of bHb-HES130 and bHb-HES200 were recorded by a UV-1800 spectrophotometer (Shimadzu, Japan). bHb-HES130 and bHb-HES200 were both at a protein concentration of 0.4 mg/mL in 20 mM sodium phosphate buffer (pH 7.4).

2.14. FT-IR Spectroscopy. bHb-HES130 and bHb-HES200 were dialyzed against water followed by lyophilization. The lyophilized samples were determined by a Nicolet iS50 FT-IR spectrometer (Thermo Fisher, USA) using KBr discs. The FT-IR spectra were recorded from 4000 to 400 cm^{-1}, and the interferograms were presented as transmittance.

2.15. Colloidal Osmotic Pressure Measurements. The colloidal osmotic pressures (COPs) of bHb-HES130 and bHb-HES200 at different protein concentrations (5−25 mg/mL) were measured by a Wescor 4420 Colloidal Osmometer at room temperature. The samples were dissolved in PBS buffer (pH 7.4). Each sample was measured three times. The instrument was calibrated by Osmocoll reference standards (Wescor).

2.16. Animals. Healthy male Wistar rats (220−260 g; Vital River, Beijing, China) were treated with ad libitum access to food and water. The rats were anesthetized by intraperitoneal injection of 50 mg/kg of pentobarbital sodium (Chinese Medicine Group Chemical Agent, Beijing, China) and placed in the supine position on a warming pad (TMS-202, Softron Biotechnology, Beijing, China) at 37 ± 0.1 °C. Heparin (400 U/kg; Chinese Medicine Group Chemical Agent, Beijing, China) was administered via the carotid artery to inhibit coagulation. All experimental procedures were approved by the Laboratory Animal Center of the Academy of Military Medical Sciences (IACUC-DWZX-2022−631, Beijing, China). The research protocol adhered to the institutional guidelines for the care and use of laboratory animals. The next studies were not performed in Wistar rats, but rather Wistar rat blood was used in vitro.

2.17. Viscosity. bHb, bHb-HES130, and bHb-HES200 were mixed with whole blood from the Wistar rats at a ratio of 1:5 (v/v) at room temperature, respectively. The supernatant was obtained by centrifugation of the mixtures at 2000 rpm for 10 min. The mixtures (500 μL) and the corresponding supernatants (500 μL) were used for the viscosity measurement. bHb, bHb-HES130, and bHb-HES200 were all in the range of 5−15 mg bHb/mL (500 μL) in 20 mM sodium phosphate buffer (pH 7.4). The viscosity was measured at a shear rate range of 50−200 s^{-1} at 37 °C using a rheometer (Brookfield Engineering, USA). Each sample was measured three times.

2.18. Index of Rigidity. The effect of bHb-HES130 and bHb-HES200 on the deformability of red blood cells could be reflected by the index of rigidity (IR).[41] IR was calculated by the following formula: $IR = (\eta_h - \eta_p)/\eta_p \times 1/Hct$. η_h was the viscosity of the whole blood. η_p was the viscosity of the mixture of the samples and whole blood at a ratio of 1:5 (v/v). The viscosity was measured at a shear rate of 200 s^{-1}. The mean value of Hct in whole blood was 41.6%. The Hct values of other groups were calculated according to the mixing ratio of the volume.

2.19. Platelet Aggregation. Two female Wistar rats (∼300 g) were anesthetized by intraperitoneal injection of 2.5% pentobarbital sodium solution. Blood was collected and placed in a tube containing 3.2% trisodium citrate. All experimental procedures were approved by the Laboratory Animal Center of the Academy of Military Medical Sciences (IACUC-DWZX-2022-631, Beijing, China). The platelet-rich plasma (PRP) was obtained by centrifuging one aliquot of the whole blood at 100g for 10 min. The platelet-poor plasma (PPP) was acquired by centrifugation of one aliquot at 2000g for 5 min.

bHb, bHb-HES130, and bHb-HES200 (10 μg bHb/μL, 15 μL) were mixed with PRP (210 μL) or PPP (235 μL) in a cuvette. The mixtures were incubated with constant shaking at 100 rpm for 15 min at room temperature. All the samples were placed in a thermostatic well of a platelet aggregometer (Helena AggRAM, USA) and incubated at 37 °C for 15 min. Distilled water was used to calibrate the instrument. The mixtures containing PPP were measured directly. The mixtures containing PRP were measured with addition of 50 μM adenosine diphosphate (ADP, 25 μL). The spectra of the aggregation percentage were recorded by HemoRam software (Version 1.3). The maximal aggregation percentage was directly obtained from the spectra, which reflected the aggregation rate of platelets.[42]

2.20. Hemolysis Rate. The red blood cells (RBCs) from the Wistar rats were washed three times using normal saline solution and centrifuged at 2000g for 10 min. bHb-HES130 and bHb-HES200 (30 μL) were mixed with RBCs (300 μL) at 30% hematocrit (Hct). The mixtures were incubated for 1 h at 37 °C to obtain the cell suspension. Each suspension (150 μL) was added with normal saline (NS) solution (400 μL). The total Hb concentration (ctHb) was measured by a BC-500 veterinary whole blood analyzer (Mindary, China). The mixtures were centrifuged at 2000g for 10 min to obtain the supernatant. Each supernatant was mixed with a chromogenic reagent and incubated for 20 min at 37 °C using a free hemoglobin assay kit. Distilled water was used as the control, and the absorbance at 510 nm was determined. Each measurement was repeated three times. The hemolysis rate was calculated by the following formula: Hemolysis rate = Free Hb concentration × (1 − Hct)/ctHb.

2.21. Blood Cell Morphology. The morphology of RBCs in the presence of bHb-HES130 and bHb-HES200 was measured using an inverted optical microscope (RVL-100-G, ECHO, USA). bHb, bHb-HES130, and bHb-HES200 (0.3 mg bHb) were incubated with BRCs at 0.6% Hct for 30 min. The specimens were prepared by dropping the mixtures (20 μL) onto the slide followed by covering with the cover glass. The specimens were observed under the inverted optical microscope. The magnification was adjusted to 40× to take a photo.

https://doi.org/10.1021/acsomega.3c00275
ACS Omega 2023, 8, 11447−11456

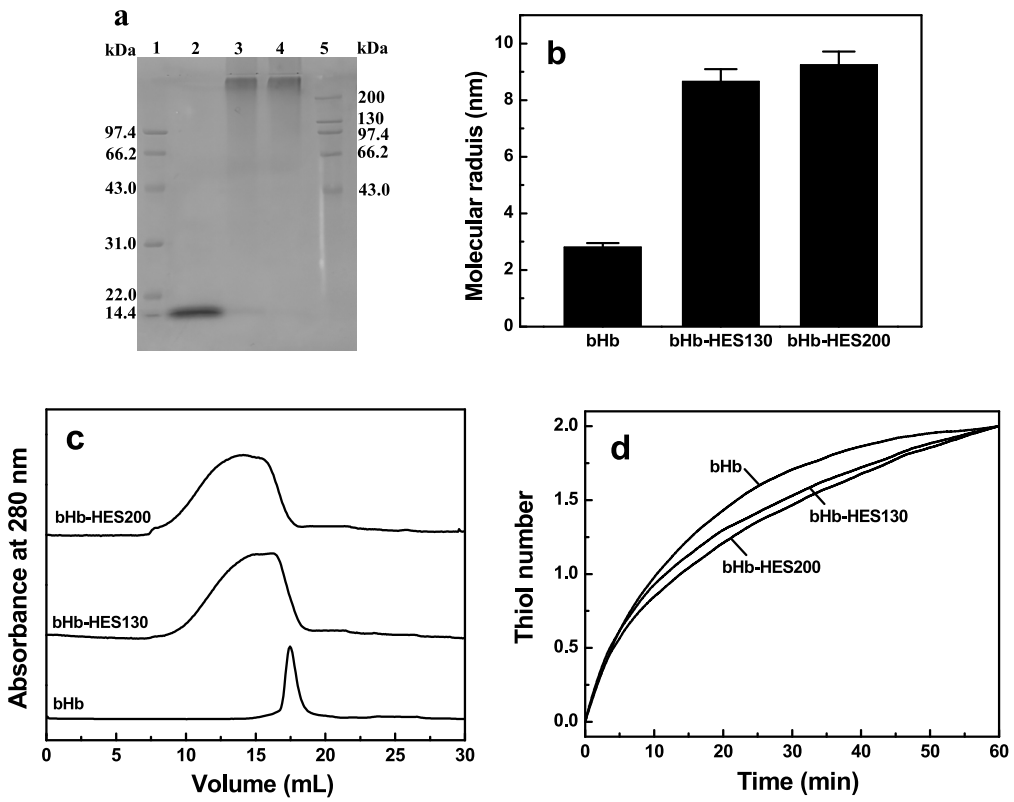

Figure 1. Analysis of bHb-HES130 and bHb-HES200. The conjugates were analyzed by SDS-PAGE (a). Lanes 1 and 5 - marker, Lane 2 - bHb, Lane 3 - bHb-HES130, and Lane 4 - bHb-HES200. The conjugates were analyzed by dynamic light scattering (b) and a Superose 6 column (c). Values represent the mean value ± SD from three repeated measurements. The thiol reactivities of the conjugates (d) were estimated by measuring the conversion of 4-PDS to 4-thiopyridone at 324 nm as a function of time.

3. RESULTS

3.1. SDS-PAGE Analysis. HES130 and HES200 were conjugated with bHb to generate bHb-HES130 and bHb-HES200, respectively. As shown in Figure 1a, bHb (Lane 2) displayed a single band corresponding to one globin of bHb (16 kDa). This was due to the dissociation of the tetrameric bHb (64 kDa) to one globin under the electrophoresis condition. bHb-HES130 (Lane 3) and bHb-HES200 (Lane 4) both exhibited a band with much lower mobility than bHb corresponding to a molecular weight of over 200 kDa. The oxidized HES contains multiple aldehyde groups, and bHb contains multiple amino groups. Multiple aldehyde groups of one HES molecule may react with the amino groups of Hb subunits. Thus, the four subunits of Hb may be intramolecularly cross-linked by the conjugated HES, which can prevent the dissociation of bHb subunits.

3.2. Dynamic Light Scattering Analysis. The molecular radii of bHb-HES130 and bHb-HES200 were determined by dynamic light scattering. As shown in Figure 1b, the molecular radius of bHb-HES130 (8.66 nm) was higher than that of bHb (2.81 nm, $P < 0.05$) and lower than that of bHb-HES200 (9.25 nm, $P < 0.05$). This revealed that the molecular radius of bHb could be significantly enhanced by conjugation with HES.

3.3. Quantitative Assay. The Hb and HES contents of the two conjugates were measured. The Hb/HES molar ratios of bHb-HES130 and bHb-HES200 were calculated to be 3.3:1 and 3.5:1, respectively. Thus, one HES molecule was conjugated with 3−4 bHb molecules in one entity. This suggested that HES could be conjugated with multiple bHb molecules and the bHb amount was comparable in the two conjugates.

3.4. Size Exclusion Chromatography Analysis. bHb-HES130 and bHb-HES200 were both analyzed by an analytical Superose 6 column (1 cm × 30 cm). As shown in Figure 1c, bHb was eluted as a single peak at 17.5 mL. In contrast, bHb-HES130 was eluted as a wide and asymmetric peak at 15.7−16.3 mL that was left-shifted compared to bHb due to the wide molecular-weight distribution of the conjugated HES130. Moreover, bHb-HES200 was eluted as a wide peak at 13.7−14.3 mL, which was left-shifted compared to bHb-HES130. This was due to the conjugation of HES200 with a larger molecular size.

3.5. Thiol Reactivity. The thiol reactivity of Cys-93(β) in the oxy state of Hb was an indicator of a structural change at the $\alpha1\beta2$ interface of Hb.[43] Thiol reactivities of Cys-93(β) in the conjugates were measured by titration with 4-PDS. As shown in Figure 1d, the thiol reactivity of bHb-HES130 was slightly lower than that of bHb and higher than that of bHb-HES200. Thus, conjugation with HES resulted in slight structural perturbation at the $\alpha1\beta2$ interface of bHb. Moreover, the thiol groups of the three samples were close to 2.0, indicating that the two thiol groups were essentially maintained in the conjugates.

3.6. Circular Dichroism Spectroscopy. The structures of the conjugates were investigated by CD spectroscopy. The L band (~260 nm) was sensitive to the interaction between the heme and the surrounding globin, being influenced by the ligand interactions. As shown in Figure 2a, the L band intensities of the conjugates were higher than that of bHb. In

https://doi.org/10.1021/acsomega.3c00275
ACS Omega 2023, 8, 11447−11456

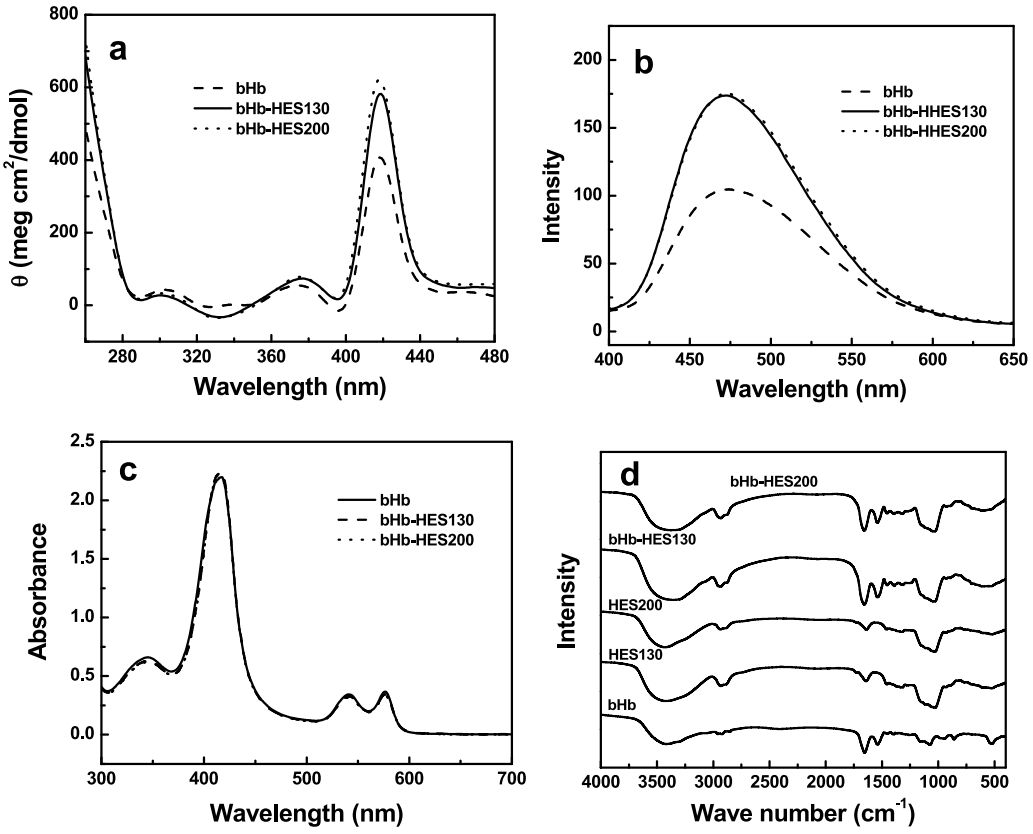

Figure 2. Structural characterization bHb-HES130 and bHb-HES200. The circular dichroism spectra (a), extrinsic fluorescence spectra (b), UV−vis spectra (c), and FT-IR spectra (d) of the conjugates were recorded.

contrast, the intensity of bHb-HES130 was slightly lower than that of bHb-HES200. This indicated that conjugation with HES altered the interaction of oxygen and the heme of bHb.[44]

A molar ellipticity of approximately 285 nm was indicative of the transition from the R (relax) state to the T (tense) state and sensitivity to the quaternary structure of Hb at the $\alpha 1\beta 2$ interface.[45] As shown in Figure 2a, the ellipticity of approximately 285 nm of bHb-HES130 was slightly lower than that of bHb and slightly higher than that of bHb-HES200. This indicated that conjugation of HES could slightly perturb the structural transition of bHb from the R state to the T state and alter the oxygen delivery and unloading of bHb.

The Soret band of Hb reflected the interactions of the heme prosthetic group with the surrounding aromatic residues and modifications in the spatial orientation of these amino acids with respect to the heme, affecting porphyrin transitions and $\pi-\pi^*$ transitions in the surrounding aromatic residues.[46] As shown in Figure 2a, the conjugates both showed higher ellipticity than bHb in the Soret band region along with no shift in the maximal wavelength of the Soret band. In addition, the ellipticity of bHb-HES130 was slightly lower than that of bHb-HES200. This suggested that conjugation with HES could slightly perturb the heme environment of bHb.

3.7. Extrinsic Fluorescence Analysis. The hydrophobicity of the conjugates was determined by extrinsic fluorescence spectroscopy using ANS as the probe.[47] As shown in Figure 2b, the spectrum of bHb-HES130 was almost superimposed on that of bHb-HES200. The fluorescence intensity of bHb was lower than those of the conjugates. This suggested that conjugation with HES altered the hydrophobicity of bHb. Moreover, bHb and the two conjugates all showed the maximum wavelength at 473 nm.

3.8. UV−Vis Spectroscopy. UV−vis spectroscopy was used to analyze the conjugates. As shown in Figure 2c, bHb showed three characteristic peaks at 410, 540, and 576 nm. The spectra of the conjugates were almost superimposed on that of bHb. The three characteristic peaks indicated that the conjugates were in the form of full oxygenation. In addition, no peak was observed at 630 nm in the spectra, which could reflect the presence of the methemoglobin. Moreover, the methemoglobin contents of the two conjugates were calculated to be zero with the absorbance at 560, 576, and 630 nm.[37]

3.9. FT-IR Spectroscopy. FT-IR spectroscopy was used to characterize the conjugates. As shown in Figure 2d, the FT-IR spectrum of bHb showed the characteristic peaks at 3300 cm^{-1} (N−H stretching), 1650 cm^{-1} (C═O stretching), and 1540 cm^{-1} (N−H wagging). The spectra of HES130 and HES200 showed the characteristic peaks at 3300 cm^{-1} (O−H stretching), 2925 cm^{-1} ($-CH_2$ asymmetric stretching), and 2851 cm^{-1} ($-CH_2$ symmetric stretching). In particular, the peaks at 2925 and 2851 cm^{-1} were ascribed to the hydroxyethyl moieties of HES. The spectra of the conjugates showed the characteristic peaks at 3300, 2925, 2851, 1650, and 1540 cm^{-1}. This indicated that the two spectra contained the signals of HES and bHb. Moreover, the intensities of the conjugates at 1540 cm^{-1} were stronger than bHb due to the formation of secondary amine groups between HES and bHb. The intensities of the conjugates at 1650 cm^{-1} were significantly stronger than bHb, indicating that the conjugates still maintained the classical α-helix of bHb.

https://doi.org/10.1021/acsomega.3c00275
ACS Omega 2023, 8, 11447−11456

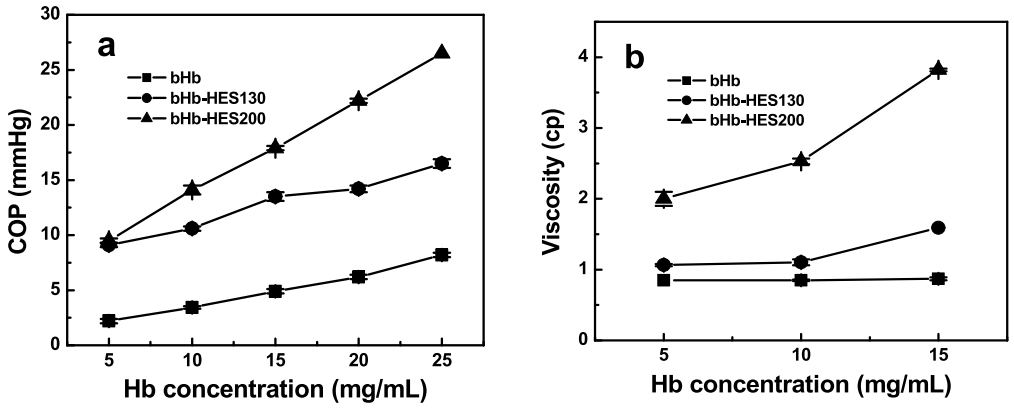

Figure 3. Colloidal osmotic pressure and viscosity of bHb-HES130 and bHb-HES200. The colloidal osmotic pressure (a) was measured using Osmocoll reference standards. The viscosity (b) was measured at a shear rate of 100 s^{-1}. Values represent the mean value ± SD from three repeated measurements.

Table 1. Effect of the Conjugates on the Blood Viscosity and Plasma Viscosity

	blood viscosity (cp)				plasma viscosity (cp)			
samples	50 s^{-1}	100 s^{-1}	150 s^{-1}	200 s^{-1}	50 s^{-1}	100 s^{-1}	150 s^{-1}	200 s^{-1}
control[a]	11.00	8.70	7.72	7.07	1.18	1.18	1.18	1.16
normal saline[b]	6.94	5.89	5.39	5.05	1.19	1.15	1.13	1.09
bHb	7.75	6.42	5.75	5.34	1.22	1.18	1.17	1.15
bHb-HES130	5.32	4.75	4.43	4.24	1.43	1.32	1.30	1.25
bHb-HES200	5.00	4.57	4.35	4.21	1.31	1.34	1.34	1.33

[a]Whole blood group. [b]Mixture of whole blood and normal saline.

3.10. Oxygen Affinity Measurement. The P_{50} values of bHb-HES130 (15.1 mmHg) and bHb-HES200 (13.9 mmHg) were both lower than that of bHb (30.2 mmHg) under physiological conditions (pH 7.4). Thus, HES conjugation could decrease the P_{50} values of bHb as a function of the HES size. However, the P_{50} values of the conjugates indicated that they still exhibited certain ability for oxygen delivery and unloading. On the other hand, the Hill coefficients (n) of bHb-HES130 (1.74) and bHb-HES200 (1.67) were lower than that of bHb (2.79), indicating that the subunit cooperativity of bHb was decreased upon conjugation with HES. Although the P_{50} and Hill coefficients decreased, the two conjugates could still provide oxygen supply to the hypoxic tissues.

3.11. Bohr Effect. The Bohr effect of bHb could be reflected by P_{50} values at the different pH conditions. The P_{50} values of bHb at pH 7.2 and 7.6 were 30.2 and 23.2, respectively, which increased as the pH decreased. In contrast, the P_{50} values of bHb-HES130 at pH 7.2 and 7.6 were 19.5 and 12.8, respectively. The P_{50} values of bHb-HES200 at pH 7.2 and 7.6 were 15.1 and 11.6, respectively. Thus, the P_{50} sensitivity of bHb-HES130 and bHb-HES200 to low pH was not altered. This indicated that the protonation effect on the oxygen affinity of bHb was not altered by HES conjugation. Thus, the Bohr effect of bHb was not altered by conjugation with HES.

3.12. Colloidal Osmotic Pressure. The COP is important to maintain the water balance between inside and outside blood vessels, which reflects the ability of a plasma expander to expand the blood volume. As shown in Figure 3a, the COP values of the conjugates increased as a function of the bHb concentration. Moreover, the COP of bHb-HES130 was higher than that of bHb and lower than that of bHb-HES200. In particular, the COP values of bHb-HES130 and bHb-HES200 at 25 mg/mL were 16.5 and 26.5 mmHg, respectively. Thus, it was expected that the conjugates could expand the blood volume and improve the blood circulation to the hypoxic tissues.

3.13. Viscosity. As shown in Figure 3b, the viscosity of bHb-HES130 was higher than that of bHb and lower than that of bHb-HES200 at 5−15 mg/mL. Thus, conjugation with HES could significantly increase the viscosity of bHb. The viscosity of bHb slightly and linearly increased as the protein concentration increased. In contrast, the viscosities of the conjugates both exhibited a non-linear dependence on the protein concentration.

As shown in Table 1, the blood viscosities of bHb, bHb-HES130, and bHb-HES200 gradually decreased as the shear rate increased. In contrast, the plasma viscosities of the samples slightly decreased as the shear rate increased. Compared with the control, dilution with NS and bHb slightly decreased the blood viscosity and essentially maintained the plasma viscosity. In contrast, dilution with the conjugates significantly decreased the blood viscosity and slightly increased the plasma viscosity.

3.14. Index of Rigidity. The deformability of RBCs is conducive to pass through capillaries and improve the microcirculation. The IR is an indicator to evaluate the deformability of RBCs, and a high IR indicated the poor deformation capacity of RBCs. The IR value of RBCs was 12.22 ± 0.15. In contrast, the IR values of RBCs incubated with NS, bHb, bHb-HES130, and bHb-HES200 were 8.71 ± 0.10, 8.74 ± 0.10, 5.74 ± 0.07, and 5.19 ± 0.06, respectively. Thus, the conjugates showed low IR values.

3.15. Hemolysis Rate. As a parameter to characterize the hemocompatibility, the hemolysis rates of the conjugates were measured. As shown in Table 2, the hemolysis rates of HES130, HES200, bHb-HES130, and bHb-HES200 were all

https://doi.org/10.1021/acsomega.3c00275
ACS Omega 2023, 8, 11447−11456

Table 2. Hemolysis Rate and Platelet Aggregation of bHb-HES130 and bHb-HES200[a]

samples	hemolysis rate (%)	platelet aggregation (%)
normal saline	0.039 ± 0.001	78.3 ± 4.8
bHb	0.046 ± 0.001	80.4 ± 0.5
HES130	0.042 ± 0.001	84.7 ± 0.7
HES200	0.031 ± 0.001	80.6 ± 2.5
bHb-HES130	0.030 ± 0.001	92.8 ± 1.8
bHb-HES200	0.042 ± 0.001	91.7 ± 1.4

[a]Values represent the mean value ± SD from three repeated measurements.

slightly lower than that of bHb. This indicated that conjugation of HES could slightly decrease the hemolysis rate of bHb. Moreover, the hemolysis rates of the conjugate groups were close to that of the NS group.

3.16. Platelet Aggregation. ADP is a main platelet activator and could process the platelet aggregation. As shown in Table 2, the platelet aggregation rates of the bHb (80.4%), HES130 (84.7%), and HES200 (80.6%) groups were close to that of NS (80.7%). In contrast, the platelet aggregation rates of the bHb-HES130 (92.8%) and bHb-HES200 (91.7%) groups were higher than that of NS (80.7%). This indicated that the conjugates could promote the ADP-induced platelet aggregation. Thus, conjugation with HES could maintain the normal hemostatic mechanism of RBC.

3.17. Morphology of RBCs. RBCs exhibited a double concave disc shape in the normal vessels. The appearance of RBCs may be altered to spinous and spherical erythrocytes by extra factors. As shown in Figure 4, there are essentially no differences among images a−f. The erythrocytes containing NS, HES, and the two conjugates were all intact and their morphological integrity was maintained. However, RBCs were attached and showed some rouleaux-like structure at the right top side in Figure 4e. The RBC adhesion of the bHb-HES130 group may be due to the fact that the sample was not fully mixed before addition to the slide. In our pre-experiment, the adhesion of RBCs in the presence of bHb-HES was observed with the extension of incubation time (0, 30, and 60 min). The increase in the bHb-HES volume did not alter this situation.

4. DISCUSSION

In the present study, HES and bHb were covalently conjugated to develop an effective oxygen carrier and plasma expander. The oxygen affinity, Bohr effect, and structure of the conjugates (bHb-HES130 and bHb-HES200) were measured to evaluate their effectiveness as an oxygen carrier. The COP and viscosity of the conjugates were investigated to evaluate their ability to compensate for the intravasal volume deficiency. The physiological effects of the conjugates on RBCs were also investigated.

HES130 and HES200 induce severe hypoxia in the tissue due to the fact that they cannot deliver and release the oxygen. In contrast, Hb could alleviate the hypoxia in the tissues for its oxygen-delivery ability. Thus, these two molecules were conjugated with Hb to achieve this objective. Previously, Sakai et al.[34] used HES with a M_w of 70 kDa to conjugate with Hb. HES was activated by cyanogen bromide followed by conjugation with Hb at harsh conditions (pH 10.8). In the present study, HES with a higher M_w (130 and 200 kDa) was oxidized by sodium periodate to obtain the aldehyde groups. The aldehyde groups of HES could react with the ε-amino groups of lysine residues and the α-amino groups of N-terminal valine residues of bHb under mild conditions (pH 7.4) to obtain the bHb-HES conjugate.

Some lysine residues (e.g., Lys-40(α)) played an important role in cooperative oxygen binding with Hb. Conjugation at these sites could perturb the T state and the heme environment of bHb thereby altering the oxygen delivery and unloading. In addition, the conjugated HES could create a large hydrated layer around bHb by binding bulky water molecules, which restricted the R state-to-T state transition of bHb. The oxy conformational state of bHb with more water molecules was thus favored over the deoxy state with less water molecules. Thus, the low P_{50} values of bHb-HES130 and bHb-HES200 could either be a direct consequence of covalent conjugation with bHb, or the conjugated HES itself, or a combination of the two. However, the P_{50} values of bHb-HES130 (15.12 mmHg) and bHb-HES200 (13.89 mmHg) were close to or in the range of 15−20 mm Hg, which could achieve adequate oxygen delivery in vivo to the tissues and alleviate tissue hypoxia.[48]

Typically, intravenous infusion of a large volume of protein solution may alter the solution properties of the blood. The COP was related to the colloidal volume-expanding efficacy and facilitated the blood flow recovery in resuscitation.[49] Previously, Hu et al. prepared a PEGylated Hb to act as an oxygen carrier and plasma expander using aldehyde chemistry.[50] The PEGylated Hb at 20 mg/mL showed a COP value

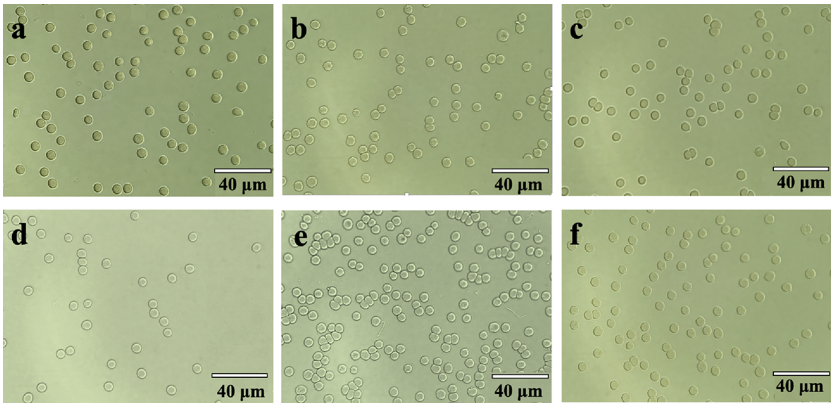

Figure 4. Morphology of RBCs in the presence of different samples. The RBCs were incubated with normal saline (a), bHb (b), HES130 (c), HES200 (d), bHb-HES130 (e), and bHb-HES200 (f), respectively.

https://doi.org/10.1021/acsomega.3c00275
ACS Omega 2023, 8, 11447−11456

of ∼30 mmHg, which was slightly higher than that of bHb-HES200 (∼22 mmHg at 20 mg/mL). Thus, conjugation of bHb with HES was expected to increase the plasma volume and the molecular volume and reduce the in vivo extravasation rates of bHb and HES.

Viscosity is an important factor for putative plasma expanders. The colloid solution exerted on the endothelial cells by flowing blood induces wall shear stress and triggers flow-induced dilation.[34] Typically, transfusion with a plasma expander could improve the blood fluidity from the interstitium and lower the whole blood viscosity and the shear stress. Interestingly, bHb-HES200 at 10 mg/mL showed a viscosity value of ∼2.4 cp, which was much higher than that of the PEGylated Hb at 10 mg/mL (∼1.2 cp).[50] Thus, the conjugate was expected to expand the blood volume and improve the microcirculation. These improved hemorheological properties can alleviate the state of anoxic tissues.

The physiological effect of bHb-HES130 and bHb-HES200 on RBCs was evaluated by measuring the RBCs morphology and rigidity, hemolysis rate, and platelet aggregation. The morphology and deformability of RBCs were maintained upon transfusion of the conjugates, which was of physiological significance for volume expansion. and bHb-HES130 and bHb-HES200 both showed good blood compatibility as reflected by the low hemolysis rates. bHb-HES130 and bHb-HES200 could maintain the normal hemostatic mechanism of RBCs. Thus, bHb-HES130 and bHb-HES200 did not display any apparent side effect on the physiological aspects of RBCs.

Significant differences in platelet aggregation of bHb-HES130/bHb-HES200 and the NS groups have been observed in our study. Previous study suggested that the HES solution had little impact on platelet aggregation.[51] In contrast, dextran sulfate triggers platelet aggregation via direct activation of PEAR1.[52] Thus, the next study should be focused on the mechanism for the conjugates to induce a strong aggregation in connection to ADP.

bHb-HES130 and bHb-HES200 both displayed unaltered Bohr effects and slight structural changes. In contrast, the P_{50} of bHb-HES130 (15.1 mmHg) was slightly higher than that of bHb-HES200 (13.9 mmHg). The COP and viscosity of bHb-HES200 were higher than those of bHb-HES130, indicating the higher ability of bHb-HES200 to compensate for the intravasal volume deficiency. Thus, bHb-HES130 showed higher ability than bHb-HES200 to act as an oxygen carrier but exhibited lower effectiveness than bHb-HES200 to work as a plasma expander.

In summary, the quaternary structure and heme environment of bHb were slightly perturbed upon conjugation with HES. The two conjugates (bHb-HES130 and bHb-HES200) could effectively deliver and release oxygen without alteration in the Bohr effect. The COP and viscosity suggested that the conjugates were an effective plasma expander. The conjugates showed no apparent side effects on the red blood cell morphology, rigidity, and hemolysis. Thus, bHb-HES130 and bHb-HES200 were expected to function as a potential oxygen carrier to alleviate tissue hypoxia and as an effective plasma expander to compensate for the intravasal volume deficiency.

AUTHOR INFORMATION

Corresponding Authors

Tao Hu − *State Key Laboratory of Biochemical Engineering, Institute of Process Engineering, Chinese Academy of Sciences, Beijing 100190, China;* orcid.org/0000-0002-6681-159X; Email: thu@ipe.ac.cn

Lian Zhao − *Institute of Health Service and Transfusion Medicine, Academy of Military Medical Sciences, Beijing 100850, China*; Email: zhaolian@bmi.ac.cn

Authors

Wenying Yan − *State Key Laboratory of Biochemical Engineering, Institute of Process Engineering, Chinese Academy of Sciences, Beijing 100190, China; University of Chinese Academy of Sciences, Beijing 100190, China*

Ming Sheng − *Institute of Health Service and Transfusion Medicine, Academy of Military Medical Sciences, Beijing 100850, China;* orcid.org/0000-0002-6824-5923

Weili Yu − *State Key Laboratory of Biochemical Engineering, Institute of Process Engineering, Chinese Academy of Sciences, Beijing 100190, China*

Lijuan Shen − *State Key Laboratory of Biochemical Engineering, Institute of Process Engineering, Chinese Academy of Sciences, Beijing 100190, China*

Jinming Qi − *State Key Laboratory of Biochemical Engineering, Institute of Process Engineering, Chinese Academy of Sciences, Beijing 100190, China*

Hong Zhou − *Institute of Health Service and Transfusion Medicine, Academy of Military Medical Sciences, Beijing 100850, China;* orcid.org/0000-0003-2987-7781

Complete contact information is available at: https://pubs.acs.org/10.1021/acsomega.3c00275

Author Contributions

#W.Y. and M.S. contributed equally to this work.

Notes

The authors declare no competing financial interest.

ACKNOWLEDGMENTS

This study was financially supported by the National Key Research and Development Project of China (no. 2018YFA0900804), Beijing Natural Science Foundation (no. L222071), and National Natural Science Foundation of China (no. 31970875).

REFERENCES

(1) Munoz, C.; Aletti, F.; Govender, K.; Cabrales, P.; Kistler, E. B. Resuscitation after hemorrhagic shock in the microcirculation: targeting optimal oxygen delivery in the design of artificial blood substitutes. *Front. Med.* **2020**, *7*, No. 585638.

(2) Cannon, J. W. Hemorrhagic shock. *N. Engl. J. Med.* **2018**, *378*, 370−379.

(3) Avery, P.; Morton, S.; Tucker, H.; Green, L.; Weaver, A.; Davenport, R. Whole blood transfusion versus component therapy in adult trauma patients with acute major haemorrhage. *Emergy Med. J.* **2020**, *37*, 370−378.

(4) Black, J. A.; Pierce, V. S.; Kerby, J. D.; Holcomb, J. B. The evolution of blood transfusion in the trauma patient: whole blood has come full circle. *Semin. Thromb. Hemostasis* **2020**, *46*, 215−220.

(5) Ware, A. D.; Jacquot, C.; Tobian, A. A. R.; Gehrie, E. A.; Ness, P. M.; Bloch, E. M. Pathogen reduction and blood transfusion safety in Africa: strengths, limitations and challenges of implementation in low-resource settings. *Vox Sang.* **2018**, *113*, 3−12.

(6) Tsai, A. G.; Vázquez, B. Y. S.; Hofmann, A.; Acharya, S. A.; Intaglietta, M. Supra-plasma expanders: the future of treating blood loss and anemia without red cell transfusions? *J. Infus. Nurs.* **2015**, *38*, 217−222.

(7) Farrugia, A. Safety of plasma volume expanders. *J. Clin. Pharmacol.* **2011**, *51*, 292−300.
(8) Chen, G.; Zhao, J.; Li, P.; Kan, X.; You, G.; Wang, Y.; Yin, Y.; Luo, X.; Zhang, Y.; Zhao, L.; Zhou, H. Effects of synthetic colloid and crystalloid solutions on hemorheology in vitro and in hemorrhagic shock. *Eur. J. Med. Res.* **2015**, *20*, 13.
(9) Yates, D. R. A.; Davies, S. J.; Milner, H. E.; Wilson, R. J. T. Crystalloid or colloid for goal-directed fluid therapy in colorectal surgery. *Br. J. Anaesth.* **2014**, *112*, 281−289.
(10) Hartog, C. S.; Bauer, M.; Reinhart, K. The efficacy and safety of colloid resuscitation in the critically ill. *Anesth. Analg.* **2011**, *112*, 156−164.
(11) Arnemann, P. H.; Hessler, M.; Kampmeier, T.; Seidel, L.; Malek, Y.; Van Aken, H.; Morelli, A.; Rehberg, S.; Ince, C.; Ertmer, C. Resuscitation with hydroxyethyl starch maintains hemodynamic coherence in ovine hemorrhagic shock. *Anesthesiology* **2020**, *132*, 131−139.
(12) Navickis, R. J.; Haynes, G. R.; Wilkes, M. M. Effect of hydroxyethyl starch on bleeding after cardiopulmonary bypass: a meta-analysis of randomized trials. *J. Thorac. Cardiovasc. Surg.* **2012**, *144*, 223−230.e5.
(13) Radhakrishnan, M.; Batra, A.; Periyavan, S.; Philip, M.; Anand, V. Hydroxyethyl starch and kidney function: A retrospective study in patients undergoing therapeutic plasma exchange. *J. Clin. Apher.* **2018**, *33*, 278−282.
(14) Boldt, J.; Suttner, S.; Brosch, C.; Lehmann, A.; Röhm, K.; Mengistu, A. Cardiopulmonary bypass priming using a high dose of a balanced hydroxyethyl starch versus an albumin-based priming strategy. *Anesth. Analg.* **2009**, *109*, 1752−1762.
(15) Hahn, R. G. Adverse effects of crystalloid and colloid fluids. *Anaesth. Intensive Ther.* **2017**, *49*, 303−308.
(16) Tiryakioglu, O.; Yildiz, G.; Vural, H.; Goncu, T.; Ozyazicioglu, A.; Yavuz, S. Hydroxyethyl starch versus Ringer solution in cardiopulmonary bypass prime solutions (a randomized controlled trial). *J. Cardiothorac Surg.* **2008**, *3*, 45.
(17) Adam, S.; Karger, R.; Kretschmer, V. Influence of different hydroxyethyl starch (HES) formulations on fibrinogen measurement in HES-diluted plasma. *Clin. Appl. Thromb. Hemost.* **2010**, *16*, 454−460.
(18) Ahmed, M. H.; Ghatge, M. S.; Safo, M. K. Hemoglobin: structure, function and allostery. *Subcell Biochem.* **2020**, *94*, 345−382.
(19) Greenburg, A. G.; Kim, H. W. Current status of stroma-free hemoglobin. *Adv. Surg.* **1997**, *31*, 149−165.
(20) Winslow, R. M. Red cell substitutes. *Semin. Hematol.* **2007**, *44*, 51−59.
(21) Habler, O. P.; Messmer, K. F. Tissue perfusion and oxygenation with blood substitutes. *Adv. Drug Delivery Rev.* **2000**, *40*, 171−184.
(22) Elmer, J.; Alam, H. B.; Wilcox, S. R. Hemoglobin-based oxygen carriers for hemorrhagic shock. *Resuscitation* **2012**, *83*, 285−292.
(23) Estep, T. N. Issues in the development of hemoglobin based oxygen carriers. *Semin. Hematol.* **2019**, *56*, 257−261.
(24) Sen Gupta, A. Hemoglobin-based oxygen carriers: current state-of-the-art and novel molecules. *Shock* **2019**, *52*, 70−83.
(25) Hill-Pryor, C.; Pusateri, A. E.; Weiskopf, R. B. Hemoglobin-based oxygen carriers (HBOC)-what the next generation holds: when red blood cells are not an option. *Shock* **2019**, *52*, 4−6.
(26) Farcas, A. D.; Toma, V. A.; Roman, I.; Sevastre, B.; Scurtu, F.; Silaghi-Dumitrescu, R. Glutaraldehyde-polymerized hemoglobin: in search of improved performance as oxygen carrier in hemorrhage models. *Bioinorg. Chem. Appl.* **2020**, 1096573.
(27) Roamcharern, N.; Payoungkiattikun, W.; Anwised, P.; Mahong, B.; Jangpromma, N.; Daduang, S.; Klaynongsruang, S. Physicochemical properties and oxygen affinity of glutaraldehyde polymerized crocodile hemoglobin: the new alternative hemoglobin source for hemoglobin-based oxygen carriers. *Artif. Cells Nanomed. Biotechnol.* **2019**, *47*, 852−861.
(28) Jahr, J. S.; Akha, A. S.; Holtby, R. J. Crosslinked, polymerized, and PEG-conjugated hemoglobin-based oxygen carriers: clinical safety and efficacy of recent and current products. *Curr. Drug Discovery Technol.* **2012**, *9*, 158−165.
(29) Li, D.; Hu, T.; Manjula, B. N.; Acharya, S. A. Non-conservative surface decoration of hemoglobin: influence of neutralization of positive charges at PEGylation sites on molecular and functional properties of PEGylated hemoglobin. *Biochim. Biophys. Acta* **2008**, *1784*, 1395−1401.
(30) Kozma, G. T.; Shimizu, T.; Ishida, T.; Szebeni, J. Anti-PEG antibodies: Properties, formation, testing and role in adverse immune reactions to PEGylated nano-biopharmaceuticals. *Adv. Drug Delivery Rev.* **2020**, *154-155*, 163−175.
(31) Wan, X.; Zhang, J.; Yu, W.; Shen, L.; Ji, S.; Hu, T. Effect of protein immunogenicity and PEG size and branching on the anti-PEG immune response to PEGylated proteins. *Process Biochem.* **2017**, *52*, 183−191.
(32) Barbier, P.; Jonville, A. P.; Autret, E.; Coureau, C. Fetal risks with dextrans during delivery. *Drug Safety* **1992**, *7*, 71−73.
(33) Baldwin, J. E.; Gill, B.; Whitten, J. P.; Taegtmeyer, H. Synthesis of polymer-bound hemoglobin samples. *Tetrahedron* **1981**, *37*, 1723−1726.
(34) Sakai, H.; Yuasa, M.; Onuma, H.; Takeoka, S.; Tsuchida, E. Synthesis and physicochemical characterization of a series of hemoglobin-based oxygen carriers: objective comparison between cellular and acellular types. *Bioconjugate Chem.* **2000**, *11*, 56−64.
(35) Perutz, M. F.; Fermi, G.; Poyart, C.; Pagnier, J.; Kister, J. A novel allosteric mechanism in haemoglobin. Structure of bovine deoxyhaemoglobin, absence of specific chloride-binding sites and origin of the chloride-linked Bohr effect in bovine and human haemoglobin. *J. Mol. Biol.* **1993**, *233*, 536−545.
(36) Manjula, B. N.; Acharya, S. A. Purification and molecular analysis of hemoglobin by high-performance liquid chromatography. *Methods Mol. Med.* **2003**, *82*, 31−47.
(37) Benesch, R. E.; Benesch, R.; Yung, S. Equations for the spectrophotometric analysis of hemoglobin mixtures. *Anal. Biochem.* **1973**, *55*, 245−248.
(38) Masuko, T.; Minami, A.; Iwasaki, N.; Majima, T.; Nishimura, S.; Lee, Y. C. Carbohydrate analysis by a phenol-sulfuric acid method in microplate format. *Anal. Biochem.* **2005**, *339*, 69−72.
(39) Ampulski, R. S.; Ayers, V. E.; Morell, S. A. Determination of the reactive sulfhydryl groups in heme protein with 4,4′-dipyridine disulfide. *Anal. Biochem.* **1969**, *32*, 163−169.
(40) Hu, T.; Li, D.; Manjula, B. N.; Brenowitz, M.; Prabhakaran, M.; Acharya, A. S. PEGylation of Val-1(α) destabilizes the tetrameric structure of hemoglobin. *Biochemistry* **2009**, *48*, 608−616.
(41) Muravyov, A. V.; Yakusevich, V. V.; Kabanov, A. V.; Petrochenko, A. S. The effect of diuretics on red blood cell microrheological parameters in female hypertensive patients. *Clin. Hemorheol. Microcirc.* **2005**, *33*, 121−126.
(42) Krause, S.; May, J.; Koslowski, H.; Heptinstall, S.; Lösche, W. Enhanced spontaneous platelet aggregation and red blood cell fragility in whole blood obtained from patients with diabetes. *Platelets* **1991**, *2*, 203−206.
(43) Kilmartin, J. V.; Hewitt, J. A.; Wootton, J. F. Alteration of functional properties associated with the change in quaternary structure in unliganded haemoglobin. *J. Mol. Biol.* **1975**, *93*, 203−218.
(44) Zentz, C.; Pin, S.; Alpert, B. Stationary and time-resolved circular dichroism of hemoglobins. *Methods Enzymol.* **1994**, *232*, 247−266.
(45) Perutz, M. F.; Ladner, J. E.; Simon, S. R.; Ho, C. Influence of globin structure on the state of the heme. I. Human deoxyhemoglobi. *Biochemistry* **1974**, *13*, 2163−2173.
(46) Hsu, M. C.; Woody, R. W. The origin of the heme Cotton effects in myoglobin and hemoglobin. *J. Am. Chem. Soc.* **1971**, *93*, 3515−3525.
(47) Bayer, M. E.; Bayer, M. H. Fast responses of bacterial membranes to virus adsorption: a fluorescence study. *Proc. Natl. Acad. Sci. U. S. A.* **1981**, *78*, 5618−5622.
(48) Winslow, R. M. Blood substitutes. *Adv. Drug Delivery Rev.* **2000**, *40*, 131−142.

https://doi.org/10.1021/acsomega.3c00275
ACS Omega 2023, 8, 11447−11456

(49) Tonnessen, T.; Tollofsrud, S.; Kongsgaard, U. E.; Noddeland, H. Colloid osmotic pressure of plasma replacement fluids. *Acta Anaesthesiol. Scand.* **1993**, *37*, 424−426.
(50) Hu, T.; Prabhakaran, M.; Acharya, S. A.; Manjula, B. N. Influence of the chemistry of conjugation of poly(ethylene glycol) to Hb on the oxygen-binding and solution properties of the PEG-Hb conjugate. *Biochem. J.* **2005**, *392*, 555−564.
(51) Schaden, E.; Wetzel, L.; Kozek-Langenecker, S.; Thaler, U.; Scharbert, G. Effect of the carrier solution for hydroxyethyl starch on platelet aggregation and clot formation. *Br. J. Anaesth.* **2012**, *109*, 572−577.
(52) Vandenbriele, C.; Sun, Y.; Criel, M.; Cludts, K.; Van Kerckhoven, S.; Izzi, B.; Vanassche, T.; Verhamme, P.; Hoylaerts, M. F. Dextran sulfate triggers platelet aggregation via direct activation of PEAR1. *Platelets* **2016**, *27*, 365−372.

https://doi.org/10.1021/acsomega.3c00275
ACS Omega 2023, 8, 11447−11456